Boehmite-Derived γ-Alumina System. 2. Consideration of Hydrogen and Surface Effects

Gianluca Paglia,[†,‡] Craig E. Buckley,[†] Terrence J. Udovic,[§] Andrew L. Rohl,*[,‡] Franca Jones,[‡] Clinton F. Maitland,[†] and Joan Connolly[†]

Department of Applied Physics and Nanochemistry Research Institute, Curtin University of Technology, Perth, WA 6845, Australia, and NIST Center for Neutron Research, National Institute of Standards and Technology, Gaithersburg, Maryland 20899-8562

Received November 18, 2003. Revised Manuscript Received March 4, 2004

A boehmite-derived gamma-alumina (γ-Al_2O_3) system was studied using various complementary techniques to examine surface area and pore size, the amount of hydrogen-containing species, the nature of hydrogen bonding environments, and the location of these species. Using small-angle X-ray scattering, the material examined was shown to have a significantly higher surface area than that typically expected for highly crystalline boehmite-derived γ-Al_2O_3. This higher surface area was associated with the presence of closed nanopores, the size of which was found to complement observations from transmission electron microscopy. More hydrogen was determined to be in the structure when measured using prompt-gamma activation analysis than indicated by loss on ignition experiments, suggesting that hydrogen-containing species other than water were also present. Neutron vibrational spectroscopy and infrared spectroscopy showed a reduction in signals associated with water and hydroxide species as the calcination temperature increased. Measurements from small-angle X-ray scattering and prompt-gamma activation analysis show that the surface area and the amount of hydrogen present reduce with increasing temperature treatment. This is associated with a reduction in the amount of amorphous material in the structure and an increase in pore and crystallite size. The evidence obtained suggests that the bulk crystalline structure is relatively well-ordered and contains no interstitial hydrogen. Hydrogen is therefore located at the pore surfaces and within amorphous regions, which themselves are located near pore surfaces.

Introduction

It is well-known that hydrogen is present at the surface of metal oxides. However, the role of hydrogen within the bulk structure of gamma-alumina (γ-Al_2O_3) is uncertain. This is an important consideration as water is a byproduct of the dehydration of boehmite, and many of the applications of γ-Al_2O_3 infer the involvement of hydrogen.[1−8] The majority of studies involving hydrogen in γ-Al_2O_3 investigated its presence at the surface and the relationship to Lewis acidity.[4−7,9−13]

The topotactic transformation of boehmite to γ-Al_2O_3 produces a well-developed pore structure, resulting in a high surface area.[14−19] The subsequent phase transformations to δ- and θ-Al_2O_3 are also topotactic and are accompanied by changes in the porous microstructure such that each phase has a characteristic microstructure. Each subsequent phase has an increased mean pore size and decreased surface area.

The literature review provided in Part 1 of this work was concerned with the crystalline bulk structure of γ-Al_2O_3.[20] Rietveld refinements showed that the pres-

* To whom correspondence should be addressed. E-mail: andrew@power.curtin.edu.au.
† Department of Applied Physics, Curtin University of Technology.
‡ Nanochemistry Research Institute, Curtin University of Technology.
§ NIST Center for Neutron Research.

(1) Tung, S. E.; Mcininch, E. *J. Catal.* **1964**, *3*, 229.
(2) Tsyganenko, A. A.; Filimonov, V. N. *Spectrosc. Lett.* **1972**, *5*, 477.
(3) Tsyganenko, A. A.; Filimonov, V. N. *J. Mol. Struct.* **1973**, *19*, 579.
(4) Knözinger, H.; Ratnasamy, P. *Catal. Rev. Sci. Eng.* **1978**, *17*, 31.
(5) Morterra, C.; Magnacca, G. *Catal. Today* **1996**, *27*, 497.
(6) Tsyganenko, A. A.; Mardilovich, P. P. *J. Chem. Soc., Faraday Trans.* **1996**, *92*, 4843.
(7) Liu, X.; Truitt, R. E. *J. Am. Chem. Soc.* **1997**, *119*, 9856.
(8) Sohlberg, K.; Pennycook, S. J.; Pantelides, S. T. *J. Am. Chem. Soc.* **1999**, *121*, 7493.
(9) Lavalley, J. C.; Benaissa, M. *J. Chem. Soc., Chem. Commun.* **1984**, 908.
(10) Zecchina, A.; Coluccia, S.; Morterra, C. *Appl. Spectrosc. Rev.* **1985**, *21*, 259.
(11) Busca, G.; Lorenzelli, V.; Escribano, V. S.; Guidetti, R. *J. Catal.* **1991**, *131*, 167.
(12) Busca, G.; Lorenzelli, V.; Ramis, G.; Willey, J. *Langmuir* **1993**, *9*, 1492.
(13) Sohlberg, K.; Pennycook, S. J.; Pantelides, S. T. *J. Am. Chem. Soc.* **1999**, *121*, 10999.
(14) Wilson, S. J. *J. Solid State Chem.* **1979**, *30*, 247.
(15) Wilson, S. J. *Mineral. Mag.* **1979**, *43*, 301.
(16) Wilson, S. J. *Proc. Brit. Ceram. Soc.* **1979**, *28*, 281.
(17) Wilson, S. J.; McConnell, J. D. C. *J. Solid State Chem.* **1980**, *34*, 315.
(18) Wilson, S. J.; McConnell, J. D. C.; Stacey, M. H. *J. Mater. Sci.* **1980**, *15*, 3081.
(19) Wilson, S. J.; Stacey, M. H. *J. Colloid Interface Sci.* **1981**, *82*, 507.

10.1021/cm035193e CCC: $27.50
Published on Web 04/20/2004

ence of hydrogen within the crystalline bulk was not likely, but more work is required to investigate this.[20,21] It was shown that within each grain in which the topotactic transformation sequence from boehmite occurs, amorphous regions exist, particularly for lower temperature γ-Al_2O_3 calcination products.[20] A considerable amount of amorphous content was also implied by Soled.[22] It is logical that hydrogen, whether in the form of water, hydroxide, or isolated protons, is likely to be present in these regions. However, the lamellar porous microstructure of γ-Al_2O_3, with reported mean pore widths of 8−10 Å and spacing between 35 and 40 Å,[14−19] creates ample surface for hydrogen species attachment. This can make it difficult to discern between surface hydrogen-containing species and possible hydrogen-containing species within the bulk. Here, the presence of hydrogen within the bulk is investigated and the following review summarizes research on this topic to date.

Several researchers since Dowden[23] have considered the presence of hydrogen, not bound in water form, within the bulk structure of γ-Al_2O_3. Proton NMR results from gel-derived alumina showed 9 mg of hydrogen per gram of alumina within the measured samples, with 36.8% residing within the bulk structure and the remainder at the surface.[24] These passive protons have been suggested to account for the catalytic properties of the transition aluminas.[1,6] Tsyganenko et al.[25] attributed O−H vibrations in infrared (IR) spectra of γ-Al_2O_3 exchanged with D_2O to protons trapped in octahedral and tetrahedral vacancies within the bulk anion lattice. This work was supported by the results of other researchers.[8,26,27]

De Boer and Houben[28] suggested a hydrogen-spinel (protospinel) structure for γ-Al_2O_3 analogous to the lithium spinel described by Kordes,[29] an approach that is supported by several other researchers.[8,25,26,30] On the basis of the protospinel description, the stoichiometric formula for γ-Al_2O_3 has been written γ-$Al_2O_3{\cdot}nH_2O$, with n reported to be between zero and 0.63.[24,28,30,31] This representation implies an excess of oxygen atoms and that γ-Al_2O_3 is a crystalline hydrate, which it is not.[8] Consideration of a protospinel structure may result in an idealized spinel structure, with no vacancies, represented by HAl_5O_8, or $Al_2O_3{\cdot}0.2H_2O$. This is the same composition that was established for tohdite.[32] Sohlberg et al.[8] proposed an alternative stoichiometric notation for protospinel γ-Al_2O_3, $H_{3m}Al_{2-m}O_3$, where $m = 2n/(n+3)$, which allows for a valid representation of the hydrogen content as opposed to the crystalline hydrate representation.

Contrary to the hydrogen-spinel-based structures reported, Zhou and Snyder[31] found only small amounts of hydrogen in γ-Al_2O_3; one OH per unit cell. From this they specifically ruled out hydrogen spinel as a structural possibility. Their finding is supported by the theoretical calculations of Wolverton and Hass[33] who found HAl_5O_8 to be thermodynamically unstable with respect to both boehmite and decomposition to an anhydrous defect spinel. Whereas Soled[22] has also provided an alternative notation to represent γ-Al_2O_3, hydrogen was considered only to be prevalent at the surface with a considerable amount of amorphous content, most likely in the form of water, being implied. A series of molecular dynamics studies by Álvarez et al.[34−36] supports postulations of a well-ordered, anhydrous, bulk structure with a defect-riddled surface containing many hydrogen species. It should be noted that Zhou and Snyder[31] performed their analysis on γ-Al_2O_3 synthesized from well-crystallized boehmite, as in the current work. This is in contrast to studies that have concluded in favor of considerable quantities of hydrogen in the structure, such as those by Pearson[24] and Wang et al.,[27] where gelatinous boehmite was the precursor. From this it becomes clear that preparation route is important to consider.

The structure of γ-Al_2O_3 is disordered and has a very small crystallite size which is difficult to determine, but it is typically reported between 80 and 90 Å.[22] A consequence of this is that it is very difficult to determine the surface area and its contribution to the total volume of the material. This has implications pertaining to the location of the hydrogen. Important contributions in understanding the microstructure have been provided by Wilson et al.[14−19] This paper is aimed at investigating the microstructure of the material and elucidating where hydrogen is located in the structure.

Here, in addition to traditional techniques, prompt-gamma activation analysis (PGAA)[37] and neutron vibrational spectroscopy (NVS)[38] are used to assess the amount and bonding of hydrogen in the structure of γ-Al_2O_3, and small-angle X-ray scattering (SAXS) is used to assess surface characteristics. To our knowledge, these techniques have not yet been used for this purpose. PGAA and NVS are bulk techniques that directly detect all hydrogen atoms within a sample. PGAA provides an absolute measurement of the amount of hydrogen present in the sample material. Because of the relatively large neutron scattering cross section for hydrogen compared to that of other elements, NVS provides the hydrogen-weighted vibrational density of states, spectroscopic information that reflects the bonding states experienced by hydrogen in the sample

(20) Paglia, G.; Buckley, C. E.; Rohl, A. L.; Winter, K.; Hart, R. D.; Hunter, B. A.; Studer, A.; Hanna, J. V. *Chem. Mater.* **2004**, *16*, 220.
(21) Paglia, G.; Buckley, C. E.; Rohl, A. L.; Hunter, B. A.; Hart, R. D.; Hanna, J. V.; Byrne, L. T. *Phys. Rev. B* **2003**, *68*, 141110.
(22) Soled, S. *J. Catal.* **1983**, 81.
(23) Dowden, D. A. *J. Chem. Soc.* **1950**, *1−2*, 242.
(24) Pearson, R. M. *J. Catal.* **1971**, *23*, 388.
(25) Tsyganenko, A. A.; Mirnov, K. S. S.; Rzhevskij, A. M.; Mardilovich, P. P. *Mater. Chem. Phys.* **1990**, *26*, 35.
(26) Saniger, J. M. *Mater. Lett.* **1995**, *22*, 109.
(27) Wang, J. A.; Bokhimi, X.; Morales, A.; Novaro, O.; Lopez, T.; Gomez, R. *J. Phys. Chem. B* **1999**, *103*, 299.
(28) de Boer, J. H.; Houben, G. M. M. *Proc. Int. Symp. React. Solids (Flanders Boktryckeri Aktieboolag, Göteburg)* **1952**, *1*, 237.
(29) Kordes, E. *Z. Kristallogr.* **1935**, *91*, 202.
(30) Ushakov, V. A.; Moroz, E. M. *React. Kinet. Catal. Lett.* **1984**, *24*, 113.
(31) Zhou, R.-S.; Snyder, R. L. *Acta Crystallogr.* **1991**, *B47*, 617.
(32) Yamaguchi, G.; Yanagida, H.; Ono, S. *Bull. Chem. Soc. Jpn.* **1964**, *37*, 752.
(33) Wolverton, C.; Hass, K. C. *Phys. Rev. B* **2001**, *63*, 024102.
(34) Álvarez, L. J.; León, L. E.; Sanz, J. F.; Capitán, M. J.; Odriozola, J. A. *J. Phys. Chem.* **1995**, *99*, 17872.
(35) Álvarez, L. J.; Sanz, J. F.; Capitan, M. J.; Centeno, M. A.; Odriozola, J. A. *J. Chem. Soc., Faraday Trans.* **1993**, *89*, 3623.
(36) Álvarez, L. J.; Sanz, J. F.; Capitán, M. J.; Odriozola, J. A. *Chem. Phys. Lett.* **1992**, *192*, 463.
(37) Paul, R. L.; Lindstrom, R. M.; Vincent, D. H. *J. Radioanal. Nucl. Chem.* **1994**, *180*, 263.
(38) Rush, J. J.; Udovic, T. J. In *EPD Congress 2002 and Fundamentals of Advanced Materials for Energy Conversion*; The Minerals, Metals & Materials Society: Warrendale, PA, 2002.

material. SAXS data can provide microstructure characteristics such as, in the case of the material examined here, specific surface area and total pore volume fraction. This can be complementary to information obtained from other techniques such as BET and TEM. It should be noted however that SAXS can measure closed porosity, which cannot be determined using BET.

Experimental Section

Materials. Powdered γ-Al_2O_3 samples were produced from the calcination of highly crystalline hydrogenated boehmite, obtained from the Alumina and Ceramics Laboratory, Malakoff Industries. Each boehmite precursor was calcined at temperatures between 500 and 900 °C, at 50 ± 5 °C intervals, in air. The heating rate was 5 °C per minute. Calcination of each sample lasted for 7 h at each temperature. After calcination the furnace was switched off and each sample was allowed to cool to room temperature.

Small-Angle X-ray Scattering. The small-angle intensities were measured with a NanoSTAR SAXS instrument equipped with a 2-dimensional detector. Scattered photons were counted with a 2-D multiwire detector over a period of 3 h. Instrumental settings were as follows: $\lambda = 1.5418$ Å (Cu Kα), sample detector distance of 65 cm, and 2θ range between 0.04 and 4.4 degrees. The raw data had the background subtracted and were radially averaged. Resulting intensities after discarding low q data points affected by the beam stop, spanned a q range between 0.01138 and 0.31287 Å^{-1} ($q = 4\pi\sin(\theta)/\lambda$).

Method of SAXS Analysis. The approach taken for analysis of the SAXS data was adopted from Spalla et al.[39] This approach allows one to determine the volume fraction, φ, of nanosized porosity and specific surface, Σ_S, of specimens in powder form. This analysis is valid when the size of the powder grains is more than 10 times the size of the porosity. Transmission electron microscopy (TEM) images of the nanoporosity and the powder grains confirmed that this was the case.[20]

The raw intensity, $I(q)$, was converted to an absolute scale, $I_1(q)$, called the "measurable" intensity. In this form, $I_1(q)$ represents the differential scattering cross section per unit volume of solid. The measurable intensity can be determined directly:[39]

$$I_1(q) = \frac{C(q)}{C_0 \Delta\Omega(q) T d_B} \tag{1}$$

where T is transmission of the powder sample and d_B is the length of solid traversed by the incident beam. This method requires measurement of the number of incident photons per second, C_0, and number of photons per second, $C(q)$, scattered into a solid angle, $\Delta\Omega(q)$. It is difficult to measure these quantities directly with the NanoStar SAXS instrument. Instead a highly cross-linked polyethylene S-2907 standard supplied from Oak Ridge National Laboratories was used to determine the measurable intensity:

$$I_1(q) = I_{abs,st} \frac{I(q)}{I_{st}} \frac{t_{st}}{t} \frac{d_{st}}{d_B} \frac{T_{st}}{T} \tag{2}$$

where $I_{abs,st}$ is the differential scattering cross section per unit volume of the standard at $q = 0.0227$ Å^{-1}, I_{st} is the average number of photons detected in time t_{st} at $q = 0.0227$ Å^{-1}, and d_{st} is the measured thickness of the standard. The solid thickness was calculated from the measured transmission, T, and the linear attenuation coefficient of the solid ($d_B = -lnT/\mu$). The use of a standard allows the measured intensity to be converted to absolute scale, eliminating the need to determine the count rate and the solid angle required in the Spalla et al.[39] method.

Using the Porod law[40] the specific surface area can then be determined with the following expression:[39]

$$\Sigma_S = \frac{1}{\rho_m} \frac{\lim_{q\to\infty} [I_1 q^4]}{2\pi\Delta\rho^2} = \frac{1}{\rho_m} \frac{K}{2\pi\Delta\rho^2} \tag{3}$$

where ρ_m is the mass density of the solid and $\Delta\rho^2$ is the scattering length density difference between the pore and solid. The specific surface area, calculated using eq 3, includes all interfacial surface area between pores and solid, plus that between the surface of the grains and air. The Porod constant, K, was determined by fitting a constant to plots of I_1q^4 vs q over appropriate ranges of q.

To calculate the pore volume fraction, scattering from the "envelopes" of the grains needs to be subtracted. The "envelopes" are conceptualized as smoothed micrometer-sized grains. After smoothing of the grain, the envelope surface is free from any small-scale structure and porosity. The measurable intensity after subtraction of scattering from the grains is denoted by I_1^{corr}. The pore volume fraction was then calculated using the following expression:[39]

$$\int_0^\infty I_1^{corr} q^2 dq = 2\pi^2 \varphi \Delta\rho^2 \tag{4}$$

I_1^{corr} is only known over a finite q range, thus, to perform this integration extrapolation of I_1^{corr} is required. At low q, I_1^{corr} was estimated by a constant value, and at high q the corrected intensity was estimated using the Porod law.[40] Pore sizes were calculated using a spherical approximation to the pore shape:

$$r = \frac{3\varphi}{\Sigma_S(1-\varphi)\rho} \tag{5}$$

where r is the pore radius. The spherical approximation was used so that comparison could be made with the BET method, which also assumes spherical pores.

Multipoint BET Adsorption Isotherm and Density Measurements. Surface area and pore distribution of γ-Al_2O_3 samples were determined using a Micrometrics 2400 instrument operated by the Australian Nuclear Science and Technology Organization (ANSTO), Sydney, Australia. Known amounts of sample were conditioned under vacuum and a temperature of 120 °C for 16 h for degassing before re-weighing and transfer to the measuring manifold. Nitrogen gas adsorption/desorption isotherms were then recorded at various pressures, followed by analysis to determine surface area and pore size.

Density was measured using a Quantachrome Helium Pycnometer. Helium was run over preweighed samples in a micro-sample container to displace the air within the samples. The sample was then re-weighed and the total volume recorded, along with a reference volume, to yield the necessary parameters for density calculation. The density was then used to calculate the pore volume fraction:

$$\varphi = 1 - \frac{\rho_m}{\rho_i} \tag{6}$$

where φ is the volume fraction, ρ_m is the measured density, and ρ_i is the ideal crystallographic density.

Transmission Electron Microscopy. TEM was performed on a JEOL 2011 instrument fitted with a LaB_6 filament and operated at 200 kV. Samples for TEM were prepared by dispersion in water and deposition on perforated carbon films on copper support grids.

(39) Spalla, O.; Lyonnard, S.; Testard, F. *J. Appl. Crystallogr.* **2003**, *36*, 338.

(40) Porod, G. General Theory. In *Small-Angle X-ray Scattering*; Glatter, O., Kratky, O., Eds.; Academic Press: New York, 1982; p 17.

Loss on Ignition. One-shot ignition-loss was performed on the γ-Al_2O_3 samples to determine the amount of hydrogen in the bulk of the sample examined here. The sample was initially heated to 200 °C for 2 h to drive off surface-adsorbed water and cooled in a desiccator. The sample was then weighed to ±1 mg precision, heated to 1200 °C for 1 h to drive off all residual hydroxyl ions from the bulk, cooled, and weighed again. The measured mass loss was then used to determine the amount of hydrogen-containing species in the material.

Prompt-Gamma Activation Analysis. Data for PGAA were collected from the γ-Al_2O_3 samples using the PGAA spectrometer at the National Institute of Standards and Technology (NIST) Center for Neutron Research (NCNR), Gaithersburg, MD. Cold neutrons were filtered through Be and Bi at 77 K and collimated using Li-6 glass. Prompt-gamma rays were detected using a high-resolution Ge gamma-ray spectrometer.

Typically, 1-g samples (~2 cm × 2 cm × 1 cm in size) were placed in Teflon pouches and predried in air at 150 °C for 2 h each. After drying, the pouches were immediately melt-sealed. Each PGAA sample was irradiated with a beam of cold neutrons for 1−2 h. The constituent elemental nuclei absorb some of these neutrons and emit prompt gamma rays, which are measured with the gamma-ray spectrometer. The energies of these gamma rays identify the neutron-capturing elements, while the intensities of the peaks at these energies reveal their concentrations within the sample. H/Al ratios were determined from the integrated intensities of the 2223 keV prompt-gamma radiation from H and the 1778 keV decay gamma radiation from Al.[28] The integrated intensity of the Al^{28} decay gamma radiation was corrected to reflect steady-state decay intensity.

Inelastic Neutron Scattering. NVS measurements were performed on each γ-Al_2O_3 sample for 24 h at low temperature (~15 K) using the filter analyzer neutron spectrometer (FANS) at the NCNR. The Cu (220) monochromator was used with horizontal beam collimations of 60′ and 40′ of arc before and after the monochromator, respectively. Hydrogen-related phonon energies over the range of 30−260 meV (1 meV = 8.065 cm^{-1}) were measured with a liquid nitrogen cooled, Be−graphite−Be composite filter analyzer. Samples of between 9 and 12 g were placed in tubular aluminum sample cells (2.5 cm diameter × 5 cm tall) and predried in air at 150 °C for 2 h each. After drying, the samples were immediately sealed with a lid, using an indium O-ring. All spectra were normalized with respect to sample mass. The resulting spectra revealed details of the vibrational motion of hydrogenous species associated with the γ-Al_2O_3 samples and reflected the bonding environment of the hydrogen involved.

Infrared Analysis. Infrared (IR) spectra were obtained on a Bruker IFS 66 instrument using the diffuse reflectance infrared Fourier transform (DRIFT) and transmission accessories. The resolution was 4 cm^{-1} for both techniques and a mercury cadmium telluride (MCT) detector was used. An aperture of 8 mm was used for DRIFT and transmission IR, with 256 and 32 scans obtained, respectively. The evanescent wave penetrates only, at most, 1 μm into the sample, and therefore, DRIFT measures predominantly surface species. Samples of KBr mixed with 2.5% γ-Al_2O_3 were prepared for both techniques, and were pelletized for transmission IR. Spectra were taken from γ-Al_2O_3 samples where surface water was driven off by heating to 200 °C for 1 h.

Results and Discussion

It is generally anticipated that the structure of transition aluminas becomes more ordered with increasing calcination temperature. This trend is expected to coincide with an increase in the bulk density, reduced surface area, increased crystallite size, and a reduced amount of amorphous content in the material. Soled[22] attributed these characteristics to the coalescence of adjacent particles (from what has been determined in this work, the particles that Soled refers to are lamellar crystallites[20]) that become bridged by terminal oxide ions. As a result the terminal oxides become incorporated within the bulk structure.

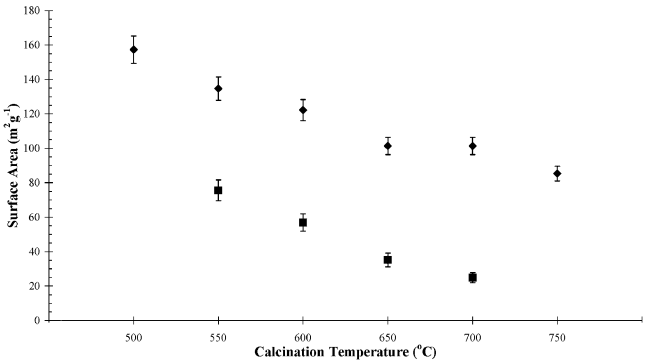

Figure 1. Specific surface area measurements from BET (■), and SAXS (◆).

The crystallite size for the material examined here has been discussed previously.[20] The crystallite size corresponds to the expected trend of increasing size with treatment temperature. The average crystallite size, as determined from analysis of the (220) peak, was ~150 Å for all samples calcined up to, and including, 750 °C, ~185 Å for samples calcined at 800 °C, and ~210 Å for samples calcined at 900 °C.

In attempting to determine if hydrogen is exclusively at the surface or if it is also located within the bulk structure, it is useful to determine the total volume of the surface and the total amount of hydrogen in the material. Figure 1 illustrates the specific surface area measurements from BET and SAXS. The decrease in surface area with increasing calcination temperature is synonymous with the coalescence of the lamellar porous microstructure. All BET surface area measurements are below 100 m^2g^{-1}, which is what is expected for γ-Al_2O_3 derived from highly crystalline boehmite.[41] The surface area measurements from BET are consistently lower than those from SAXS. Gas adsorption measurements have been shown to incompletely fill pores smaller than ~10 Å.[18,19] Higher surface areas from SAXS obviously imply large internal surfaces and very small crystallites.

Preliminary inspection of the SAXS curves (Figure 2) shows there is structure on two length scales within the sample. This is consistent with the observed micrometer-sized envelope structure of the grains and nanosized porosity within the grains.[20] Also evident from the curves in Figure 2 is that the temperature at which the sample is calcined clearly affects the nanostructure of the sample. We see that as the temperature increases, the q value at which the pore scattering becomes significant decreases. This suggests that the pore size is increasing with temperature.

The Porod plots (Figure 3) show significantly increased measured intensities at high q for samples calcined between 650 and 750 °C. In these cases, K was calculated from the plateau in the local minimum of $I_1(q)q^4$. The method used here for the determination of K follows that of Schaefer et al.[42] The consequence of this is that any short-scale structure is averaged out of the calculations, which may lead to an underestimation

(41) Wefers, K.; Misra, C. *Oxides and Hydroxides of Aluminum*; Technical Paper No. 19; Alcoa Laboroatories: Pittsburgh, PA, 1987.

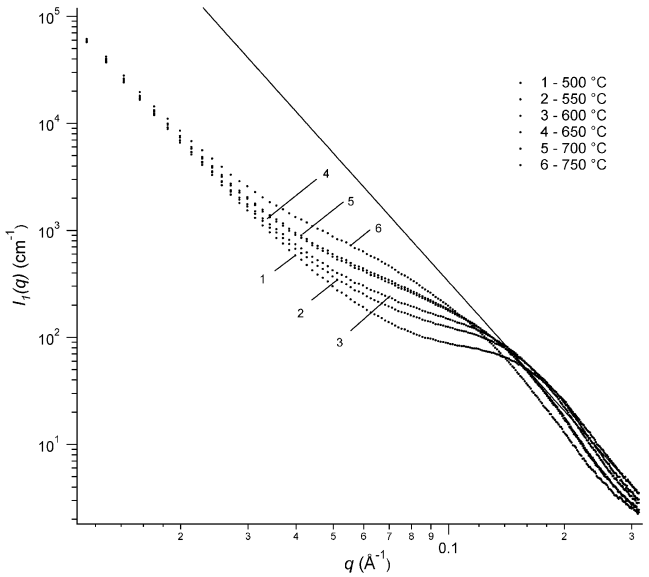

Figure 2. Intensities of the samples calcined at different temperatures as measured by SAXS. These plots clearly show that the calcination temperature affects the nanostructure. The line shows scattering that is proportional to q^{-4}.

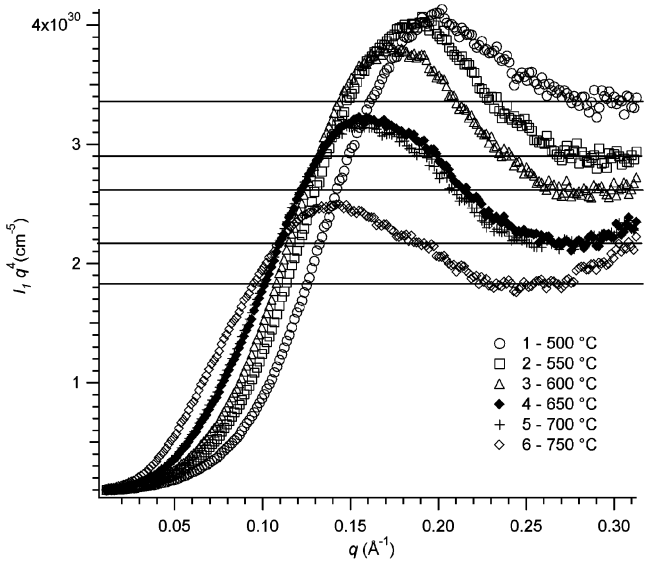

Figure 3. Porod plots of the measured intensities. The lines show the fitted values obtained for K.

of the actual specific surface area for these particular samples. Using this analysis, we are essentially probing porosity of about 20 Å in size. The increase of $I_1(q)q^4$ at high q suggests that some small porous structure ($r <$ 10 Å) remains in these samples.

From similar lamellar porous microstructures observed by Wilson et al.,[14−16] the mean pore widths were determined to be between 8 and 10 Å. From this observation it was determined that the internal surface area of γ-Al_2O_3 derived from highly crystalline boehmite can theoretically be as high as 560 m^2 g^{-1}.[19] Whereas it is clear from TEM that the microstructure is lamellar porous with nanosized pores (Figure 4), we believe it a difficult task to readily measure pore sizes from the electron micrographs, particularly in the size range specified by Wilson et al.[14−16] All that can be confidently said from the images in Figure 4 is that the lamellar shaped pores clearly have dimensions smaller than 40 Å, with pore widths smaller than the pore lengths. These observations are complementary with the SAXS data, which accounts for pore dimensions around 20 Å. This is in contrast to the BET measurements performed here which returned mean pore sizes over 45 Å for all material calcined below 750 °C. The SAXS technique also detects closed pores within the grains that cannot be measured by nitrogen gas adsorption. It is therefore concluded that γ-Al_2O_3 derived from highly crystalline boehmite has a significantly higher surface area than that measured by BET, due to the presence of closed pores.

The calculated pore volume fractions determined from SAXS analysis of the γ-Al_2O_3 samples showed a constant trend, with values between 0.16 and 0.20. This agrees well with the values obtained from pycnometry of between 0.19 and 0.20. The constant pore volume, coupled with the trend of reduced surface area, suggests that the pores are fusing together during calcination and that increased calcination temperature promotes greater fusion of pores as the bridging of crystallites progresses.[22] Figure 5 confirms this, showing increased mean nanopore dimensions with increasing calcination temperature, as the pores fuse together to yield lower surface areas, while the crystallites bridge together and increase in size. The calculated pore sizes from SAXS are between two and three times smaller than those obtained from BET. This is due to the combination of differences in measured specific surface and porosity. The calculations for pore dimension assume a spherical shape to the pores. From TEM we see that the pores are generally lamellar in shape, which is difficult to model. However, the spherical approximation was used so that the calculated sizes from BET and SAXS can be compared and is sufficient to provide an indication of relative trends that are occurring. Given the small change in pore size from 22 to 43 Å for the γ-Al_2O_3 samples calcined at different temperatures between 500 and 750 °C, it is understandable that there is no discernible difference in the microporous (nanoporous) structure when observed by TEM.[17,20] The small changes in pore size as they become fused together enables the pore morphology to remain the same.[43,44] The surface area and pore measurements are consistent with observations that the smallest pores contribute the major part of large specific surface areas.[41] A more detailed SAXS analysis on the material examined here is presented elsewhere.[45]

The lamellar pores result from the loss of water, during boehmite dehydration, from the isovolumetric environment of the grain. The stoichiometric reaction of the boehmite to γ-Al_2O_3 transformation

$$2\gamma\text{-AlOOH} \rightarrow \gamma\text{-}Al_2O_3 + H_2O \qquad (7)$$

indicates that one-quarter of the oxygen sublattice is

(42) Schaefer, D. W.; Brow, R. K.; Olivier, T. R.; Beaucage, G.; Hrubesh, L.; Lin, S. Characterisation of Porosity in Ceramic Materials by Small-Angle Scattering. In *Modern Aspects of Small-Angle Scattering*; Brumberger, H., Ed.; Kluwer Academic Publishers: Dordrecht, The Netherlands, 1995; p 299.

(43) De Boer, J. H.; Lippens, B. C. *J. Catal.* **1964**, *3*, 38.
(44) Lippens, B. C.; De Boer, J. H. *J. Catal.* **1964**, *3*, 44.
(45) Maitland, C. F.; Connolly, J.; Paglia, G.; Buckley, C. E. Manuscript in preparation.

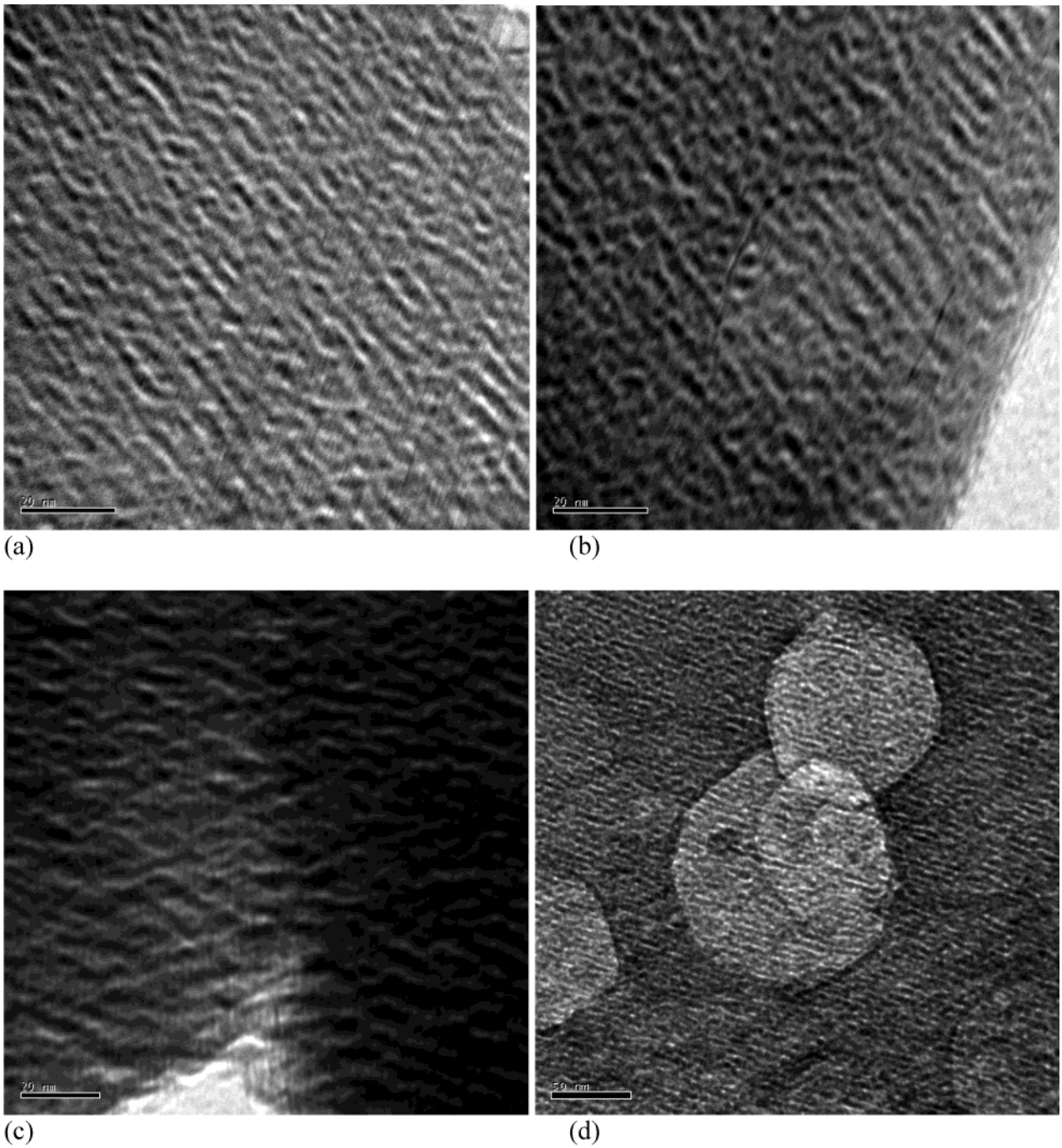

Figure 4. TEM images showing the lamellar porous microstructure: (a) and (b) γ-Al_2O_3 formed from boehmite calcined at 500 °C; (c) and (d) γ-Al_2O_3 formed from boehmite calcined at 600 °C.

lost during dehydration.[18] Consequently the total possible pore volume fraction is 0.25. Comparison with the pore volume fractions measured by SAXS and pycnometry indicates that water and amorphous material[20] fill up some of the pores.

The key question is where in the structure are the hydrogen-containing species and in what quantity? It is generally anticipated that hydrogen-containing species are located predominantly at the surface. Determining the contribution of the surface to the total volume can provide a useful indication of where hydrogen can freely reside. The volume contribution of the surface is determined from the product of the surface area, the surface layer thickness (assumed to be 1.2 Å), and the crystallographic density.[31]

e.g., at 500 °C, % volume of surface =
$(1.57 \times 10^6) \times (1.2 \times 10^{-8}) \times (3.66) \times 100 = 6.9\ \%$

The estimates are reported in Table 1. Occupation of the 32*e* site positions by Al ions in the Zhou and Snyder[31] structural model was suggested to account for the perceived large contribution to the total volume of the surface for highly crystalline boehmite-derived γ-Al_2O_3. However, the estimates provided in Table 1 show that surface volume is not significant and hence does not affect the average bulk structure. Furthermore, the suggestion of the 32*e* site position cannot account

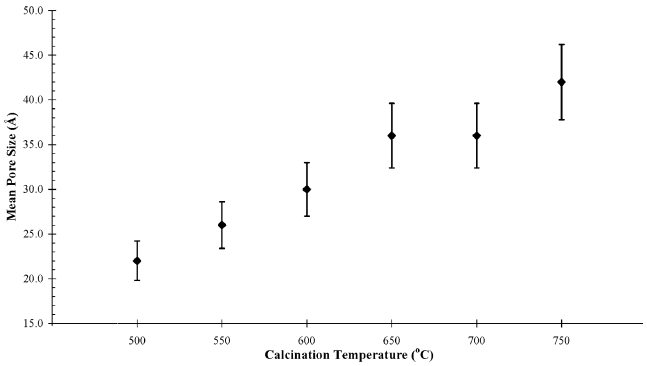

Figure 5. Mean pore diameter obtained from SAXS.

Table 1. Calculated Contribution of the Surface to the Total Volume

calcination temperature (°C)	Σ_S (m^2g^{-1})	% volume of surface
500	157 ± 8	6.9
550	135 ± 7	5.9
600	122 ± 6	5.4
650	101 ± 5	4.4
700	101 ± 5	4.4
750	85 ± 4	3.7

for the immense complexities of the γ-Al_2O_3 surface, where, in addition to the traditionally assumed three- and five-coordinated aluminum ions, four-,[46−48] six-, and seven-[34] coordinated aluminum ions have also been reported to exist.

To gain an indication of the quantity of hydrogen species that can be held by the surface, a first-order approximation can be made. If monolayer coverage of the entire surface with water is assumed, and each water molecule is assumed spherical with radius 1.1×10^{-10} m, the surface can hold up to 4.1×10^{21} molecules of water at 500 °C, which equates to 12.3 wt. %. This is a substantial amount, greater than the quantities measured from ignition-loss below. The nature of bonding interactions of hydroxide and water groups to the surface of γ-Al_2O_3 is more complicated than this and has been discussed elsewhere in more detail.[4−7,9−13]

Measuring the Quantity of Hydrogen in the Structure. The quantity of hydrogen species measured within the structure from ignition-loss measurements and PGAA is presented in Figures 6 and 7. The amount of water burnt off the surface of the samples before performing ignition-loss was also measured (Figure 6). These values are not absolute as the amount of water adsorbed onto the surface of the γ-Al_2O_3 calcination products increased rapidly with time when removed from the desiccator. However, all samples were treated identically and measurements were taken under the same conditions. Hence, the values obtained represent the relative difference in surface water adsorbed for the samples obtained here. The reduction in the amount of adsorbed surface species with increasing calcination temperature is consistent with the trend in specific surface area; there is less available surface for adsorbing species to adhere to.

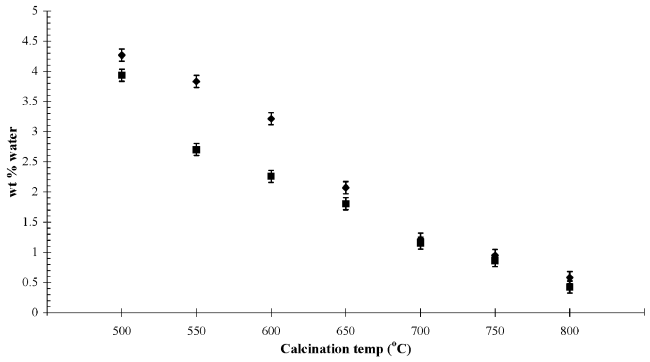

Figure 6. Ignition-loss data representing the amount of water contained within the bulk (■) and at the surface (◆) of γ-Al_2O_3 samples.

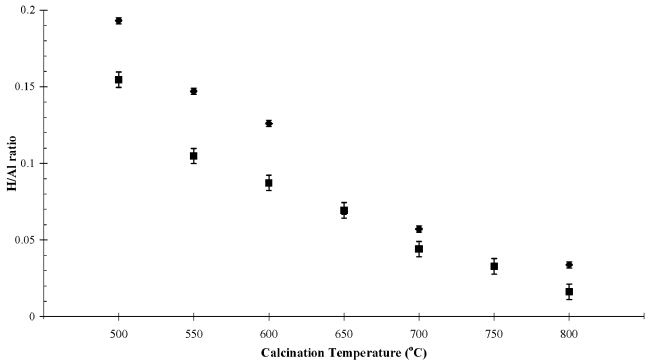

Figure 7. Ignition-loss data represented as H/Al ratios (■) compared with PGAA data (◆) of γ-Al_2O_3 samples.

The reduction of hydrogen-containing species within the bulk structure, from 3.9 wt. % at 500 °C to 0.4 wt. % at 800 °C, indicated by ignition-loss, follows a trend similar to that of the surface species. The determined quantities represent material present in amorphous regions, closed pores, and possibly, crystalline regions. Comparison of the ignition-loss data to that from PGAA (Figure 7) shows that ignition-loss underestimates the total quantity of hydrogen. This is because ignition-loss calculations assume all the material burnt off is composed solely of water. The higher proportion of hydrogen indicated by PGAA suggests the presence of hydroxide and protons, which are not burnt off within the bulk structure in addition to the water.

In addition to higher calcination temperatures, duration of heat treatment was found to affect the amount of hydrogen-containing species in the material.[14,17,18] This was measured at 550 °C with a H/Al ratio of 0.153(1) after calcination for 4 h, 0.147(1) after 7 h, and 0.136(1) after 10 h.

Rietveld analysis shows that the presence of hydrogen interstitially within the crystalline bulk structure of γ-Al_2O_3 is unlikely.[20,21] This suggests that the presence of protons in the structure, as suggested above, is limited to amorphous regions, which, in addition to hydrogen-containing species, is expected to be comprised of amorphous Al_2O_3 and other AlO species of varying stoichiometries. Protons diffuse through the structure as boehmite is broken down during the transformation to γ-Al_2O_3.[14,50] The unit cell of γ-Al_2O_3 is formed from remaining skeletal oxygen layers after the hydroxide

(46) Coster, D.; Blumenfeld, A. L.; Fripiat, J. J. *J. Phys. Chem.* **1994**, *98*, 6201.
(47) Kao, H.-C.; Grey, C. P. *J. Am. Chem. Soc.* **1997**, *119*, 627.
(48) Maresca, O.; Allouche, A.; Aycard, J. P.; Rajzmann, M.; Clemendot, S.; Hutschka, F. *J. Mol. Struct. (Thermochem)* **2000**, *505*, 81.

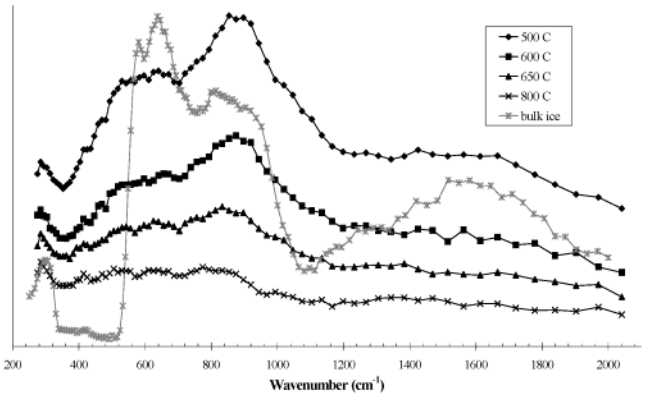

Figure 8. Normalized NVS data collected after predrying to drive off surface water for boehmite calcined between 500 and 800 °C and bulk ice.

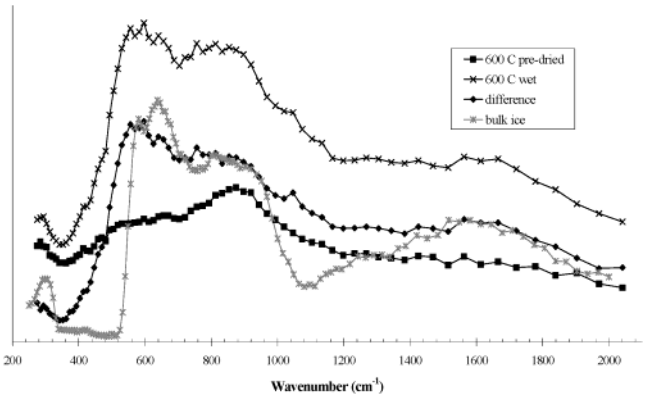

Figure 9. Illustration of the difference between the NVS spectra of predried and nonpredried (wet) samples of γ-Al_2O_3. This example was taken from boehmite calcined at 600 °C.

layers of the boehmite precursor are broken down.[14,17,51] To maintain charge neutrality, there is a counter migration of one Al into the inter-skeletal layer regions[20,51] for every three protons ejected. The hydrogen is ejected from the broken down regions, which become pores. As these regions break down, the local material forms a melt that becomes the amorphous content from which future crystalline Al_2O_3 nucleates. Protons would, therefore, be concentrated within these regions, as suggested by Rietveld analysis.[20,21] The results from ignition-loss and PGAA indicate that higher temperature or longer periods of heat treatment are required to maximize proton migration out of the pores and nearby amorphous regions through the bulk to the outer surfaces.

Neutron Vibrational Spectroscopy. Direct insight into the nature of how hydrogen, quantified above, is bonded and where it is located is provided by NVS. Figure 8 contains NVS spectra collected from several γ-Al_2O_3 samples, and bulk ice for comparison. The spectra for γ-Al_2O_3 contain two broad hydrogen-related phonon bands reflecting hydrogen bonding interactions in the structure and a third signal, at 293 cm^{-1}, which is mainly due to an Al phonon from the sample can.

The total signal for all the normalized spectra is greatest for the 500 °C sample. At 500 °C there is a significant amount of molecular water in the sample, indicated by the broad H−O−H scissor-mode band centered around ∼1600 cm^{-1}. There is also a strong, complex O−H bending mode band between 320 and 1120 cm^{-1} that decreases with increasing calcination temperature. These complex bands relate to combinations of OH and nonbulk H_2O. The difference in the shape of the NVS spectrum at 500 °C compared with the spectrum for bulk ice (Figure 8) suggests different bonding environments. Bulk ice has sharper edges due to its well-defined hydrogen bonding network. The 500 °C spectrum has broader features due to hydrogen bonding interactions between H_2O and Al_2O_3 surfaces, other H_2O molecules and OH, and the additional presence of OH groups. The broadened scissor-mode band for the 500 °C sample can also mean very small nonbulk ice configurations.

It can be assumed that the water that remains in the sample is trapped inside pores and within amorphous regions, as suggested above. The molecular water contribution to the spectra decreases with increasing temperature. By 650 °C its presence is negligible and by 800 °C it is almost nonexistent. This is signified by the reduced intensity in the spectra and the disappearance of the H−O−H scissor-mode. By 800 °C, when the transformation to γ'-Al_2O_3 is complete,[20] the main signals remaining are the complex bands between 320 and 1120 cm^{-1}, which have significantly reduced intensity and are associated with residual surface hydroxyl groups. Although possible vibrational modes from hydrogen occupying interstitial sites may be hidden by the complex O−H bending mode signals, it is more likely that the protons are not located in interstitial octahedral and tetrahedral sites within the bulk structure.

The reduction of the overall signal intensity with increasing calcination temperature is synonymous with not only a reduction in the associated molecular species with each signal, but also a reduction in amorphous content (and surface area). These results complement the observation of amorphous regions in transmission electron micrographs that were also found to decrease with increasing calcination temperature, and reduced background contributions from neutron diffraction data.[20] Soled[22] suggested that the existence of considerable amorphous content results in nonpure γ-Al_2O_3. We agree with the existence of amorphous material, but believe that the bulk crystalline structure has Al_2O_3 stoichiometry and contains no interstitial hydrogen. This belief is based on Rietveld analysis indicating that the presence of hydrogen within the crystalline bulk is unlikely.[20,21,49] Molecular dynamics simulations have also indicated that the bulk structure of γ-Al_2O_3 contains no hydrogen, is relatively well organized, and has few defects.[34−36] Given the evidence that hydrogen-containing species are present in the structure it can be deduced that there must be amorphous regions to account for these species. The amorphous nature is also evidenced by the absence of a well-defined hydrogen bonding network when the Al_2O_3 spectrum is compared to that of bulk ice.

Figure 9 illustrates the difference between the NVS spectra of predried and nonpredried (wet) samples, with boehmite calcined at 600 °C used as the example. The plot of the difference between the predried and wet

(49) Paglia, G.; Rohl, A. L.; Buckley, C. E.; Gale, J. D. Manuscript in preparation.
(50) Tsuchida, T.; Furuichi, R.; Ishii, T. *Thermochim. Acta* **1980**, *39*, 103.
(51) Lippens, B. C.; de Boer, J. H. *Acta Crystallogr.* **1964**, *17*, 1312.

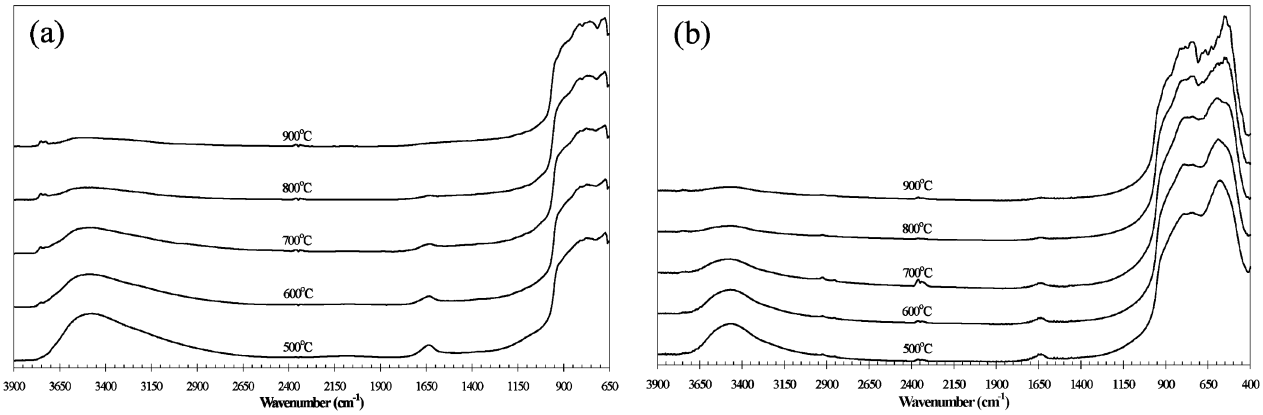

Figure 10. (a) DRIFT and (b) transmission IR spectra collected after surface water was driven off for boehmite calcined between 500 and 900 °C.

samples more dramatically shows the spectrum of only the excess water. The surface water provides a large contribution to the total signal. Comparison with the bulk ice spectrum indicates a nonbulk characteristic to the water (as per the predried samples), evidenced by the broader features of the difference plot, which signify H_2O bonding interactions with the hydroxylated Al_2O_3 surface. However, the relative signal intensities and positions in the difference plot and the clear appearance of the H−O−H scissor mode band indicate more obvious similarities of the surface water to the bulk ice spectrum, indicative of the relative quantity of molecular water at the surface. As the calcination temperature increases the difference between the predried and wet spectra diminishes.

Infrared Analysis. Comparison between DRIFT and transmission IR analysis was used to further investigate the location of hydrogen in the structure. Figure 10 shows DRIFT and transmission IR spectra for samples with physisorbed surface water driven off. Vibrational frequencies below ∼1000 cm^{-1} represent Al−O interactions in the bulk structure. It has been established that AlO_6 octahedra and AlO_4 tetrahdra are characterized by vibrational frequencies in the ranges 500−700 and 700−900 cm^{-1}, respectively.[52] The spectra also exhibit an O−H stretching mode, associated with water and hydroxide species, and an H−O−H scissor mode, associated with water species, centered at ∼3470 and ∼1620 cm^{-1}, respectively. The signal obtained for the transmission IR spectra predominantly comes from the bulk structure but there is some contribution from the surface. The signal for the DRIFT spectra originates predominantly from the surface, evidenced by the relatively smaller intensity of Al−O vibrations compared to those from transmission IR.

To investigate whether the spectra obtained could provide information about the location of hydrogen, peak intensity ratios between the AlO_6 and the O−H stretch signals, and the AlO_6 and H−O−H scissor modes, respectively, were measured. O−H/AlO_6 and H−O−H/AlO_6 ratios obtained from the DRIFT spectra were, on average, 2.5 times larger than those obtained from transmission IR spectra. The relatively more intense O−H and H−O−H signals from DRIFT indicate that the majority of hydrogen-containing species lie at the surfaces of the material examined.

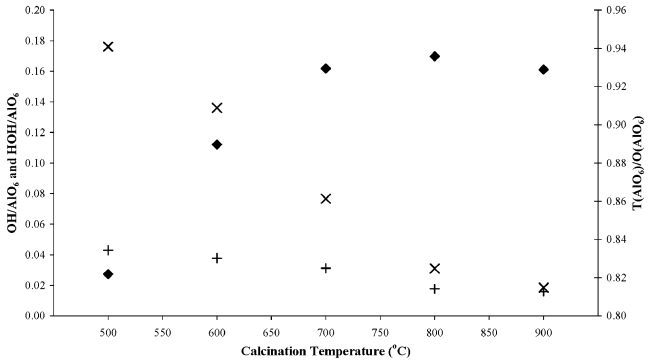

Figure 11. O−H/AlO_6 (×), H−O−H/AlO_6 (+), and AlO_4/AlO_6 (♦) ratios determined from transmission IR data.

The decrease in the intensity of O−H stretch and H−O−H bending mode signals with increasing calcination temperature (Figures 10 and 11) coincides with the trend in reduced surface area and therefore less access for attachment of hydrogen-containing species. At 800 and 900 °C, when the structure is that of γ'-Al_2O_3,[20] the O−H stretch remains present. Because the majority of the water has been ejected from the structure we can see that most of this is associated with OH at the surface.

It follows that, because the hydrogen-containing species lie at or near the surface, this is also the case for amorphous regions, as suggested earlier. Further support of amorphous regions lying at or near the surface is provided in Figure 11, which shows a decrease in the O−H/AlO_6 and H−O−H/AlO_6 ratios with increasing calcination temperature, following a trend similar to those of the PGAA and ignition-loss experiments (Figures 6 and 7).

The reduction in amorphous material in the structure is also signified by the increased sharpness, with increased calcination temperature, of the signals originating from the Al−O vibrations. Increased signal sharpness also coincides with the increased structural ordering that occurs as the transition alumina sequence evolves.[5,41,53]

Figure 11 also shows that IR data can provide an indication of the relative proportion of cations in octahedral and tetrahedral coordinated sites, when used in conjunction with other techniques. The AlO_4/AlO_6 ratio

(52) Tarte, P. *Spectrochim. Acta* **1967**, *23A*, 2127.

(53) Baraton, M. I.; Quintard, P. *J. Mol. Struct.* **1982**, *79*, 337.

increases to 750 °C, remains level to 800 °C, and then decreases slightly at 900 °C. The increase in the ratio coincides with trends of increased vacancy ordering observed in electron diffraction patterns, which represent an increase in the number of cations occupying tetrahedral site positions.[14,17,20] At 800 and 900 °C, the AlO_4 and AlO_6 peak shapes become more complex, and the position of the highest adsorption feature shifts because the IR signal is now representative of a different phase, γ'-Al_2O_3 in this case. The leveling off and decrease in the AlO_4/AlO_6 ratios coincides with the vacancy ordering on octahedral sites that occurs for transition phases beyond γ-Al_2O_3.[14,17,20] The observed trend in the AlO_4/AlO_6 ratio also corresponds to the trends found in cation occupancy, as determined from Rietveld refinements on neutron diffraction data obtained at room temperature for the same material.[20]

Conclusions

Systematic research was conducted on boehmite-derived γ-Al_2O_3 to obtain information on the types of hydrogen-containing species present and their possible location within the material. The use of SAXS, PGAA, and NVS in conjunction with the traditional techniques utilized provides a more complete picture of the role of hydrogen in the material. Specific surface area measurements, traditionally measured using nitrogen adsorption techniques, were undertaken with SAXS which indicates that the material examined has a significantly higher surface area than expected for highly crystalline boehmite-derived γ-Al_2O_3. The higher surface area was attributed to the presence of nanopores and closed porosity, where hydrogen-containing species can also be present. Expectedly, the specific surface area was found to decrease with increasing calcination temperature. This trend occurred concurrently with an increase in the mean pore and crystallite size and a reduction in the amount of hydrogen-containing species within the structure.

Loss-on-ignition experiments, based on the assumption that all hydrogen-containing species driven from the structure are lost in the form of water, were found to underestimate the amount of hydrogen in the material when compared to PGAA. The difference in the measured values is attributed to the presence of hydrogen-containing species other than water, such as hydroxide and protons. Two signals pertaining to water and hydroxide species were identified using NVS. NVS provided evidence of a reduced amount of amorphous species with increasing calcination temperature, complementing observations made from TEM and neutron diffraction patterns in part 1 of this paper.[20]

From the mechanism of γ-Al_2O_3 formation from boehmite, the hydrogen-containing species are expected to reside in the vicinity of pores, which make up the bulk of the surface area. Because the pores are remnants of broken down hydroxide layers from boehmite, the amorphous regions are also expected to be located around such regions. This is supported by infrared analysis, where the OH/AlO_6 and $H-O-H/AlO_6$ ratios obtained from the DRIFT spectra are 2.5 times larger than those obtained from transmission IR spectra, which indicates that the majority of hydrogen-containing species, and hence amorphous regions, lie at the surface of the material examined.

It can be concluded from the results obtained here that γ-Al_2O_3 derived from highly crystalline boehmite has a relatively well ordered bulk crystalline structure which contains no interstitial hydrogen and that hydrogen-containing species are located at the surface and within amorphous regions, which are located in the vicinity of pores. There is no evidence either way to suggest that hydrogen does not exist interstitially in crystalline alumina regions near the surface. We would not be surprised if this were the case, as diffusion of protons is required to maintain charge neutrality and would occur along surface regions, particularly as the amorphous regions crystallize and become more sparse. More work is required to examine this aspect.

Acknowledgment. G.P. thanks the Australian government for financial support for this research. G.P. is also grateful to the Australian Institute of Nuclear Science and Engineering (AINSE) for the provision of access to the facilities at ANSTO and additional financial support. G.P. also thanks the Western Australian Interactive Virtual Environments Centre (IVEC) for further support. C.B. acknowledges the financial support of the Australian Research Council for REIF grant R00107962 2001, which enabled the SAXS studies to be undertaken. J.C. is supported by a fellowship from the Australian Nuclear Science and Technology Organization and the Western Australian Petroleum Research Centre. Special thanks to David Cassidy, of ANSTO, for performing the BET and pycnometry, and Dr. Robert Hart and Karsten Winter, of Curtin University of Technology, who provided valuable assistance and very useful advice. Thanks to John Cornell of Alcoa World Alumina, Western Australia, for providing hydrogenated boehmite powder.

CM035193E